Plasma expansion dynamics in reactive and inert atmospheres during laser ablation of Bi(2)Sr(2)Ca(1)Cu(2)O(7−y)

J. Gonzalo, F. Vega, and C. N. Afonso

Citation: J. Appl. Phys. **77**, 6588 (1995); doi: 10.1063/1.359068
View online: http://dx.doi.org/10.1063/1.359068
View Table of Contents: http://jap.aip.org/resource/1/JAPIAU/v77/i12
Published by the American Institute of Physics.

Plasma expansion dynamics in reactive and inert atmospheres during laser ablation of Bi(2)Sr(2)Ca(1)Cu(2)O(7−y)

J. Gonzalo, F. Vega, and C. N. Afonso[a)]
Instituto de Optica, CSIC, Serrano 121, 28006 Madrid, Spain

(Received 18 November 1994; accepted for publication 16 February 1995)

The dynamics of the species ejected by excimer laser ablation of a BiSrCaCuO target in different gas environments is studied by spatially resolved, real-time optical emission spectroscopy. The evolution of the velocity and the emission intensity of the excited species versus the distance and the pressure of the foreign gas present a similar behavior both in reactive (oxygen) and inert (argon) environments. Furthermore, the results show that the plume expansion process is dominated by the interaction of the ejected species and the gas background atoms or molecules through collisional interactions rather than by reactions in the gas phase. The dynamics of the plume expansion is analyzed in the frame of the shock wave and drag models, the latter leading to a very good agreement with the experimental results and the dependence of the slowing coefficient with the gas pressure is established. Finally, the influence of the excitation energy of the considered transition on the observed emission features is discussed. © *1995 American Institute of Physics.*

I. INTRODUCTION

The possibility of growing stoichiometric superconductor films with good crystalline quality has generated an effort with no precedents in the study of the basic mechanisms of pulsed laser deposition. Since the first report of Dijkkamp *et al.*[1] on the successful deposition of YBaCuO superconducting films, many efforts have been done in order to optimize the experimental parameters that influence the quality of the deposited films, such as the target composition, the laser wavelength and energy density, and the pressure and nature of the background gas in the deposition chamber.[2–4]

Although the experimental conditions to deposit good quality high-T_c superconductor films have been established within the last few years, some questions about the nature of the process remain not yet well understood. In general the best films are deposited in an oxygen environment and, therefore, the knowledge of the interaction processes between the ablated material and the oxygen atoms or molecules seems to be essential for improving the superconducting film properties.[2–7] It is also not clear if the incorporation of oxygen takes place via the formation of oxidized species in the plume and/or by direct oxygen absorption by the growing film.[4,8] The formation of oxidized species in the gas phase during ablation of YBaCuO targets has been widely reported.[4,5,7,9] Nevertheless, no clear evidence of their formation has been given up to date in the case of ablation of BiSrCaCuO targets.

The aim of this work is to study the plume expansion dynamics during the ablation of BiSrCaCuO targets in different gas environments, in order to analyze the interaction processes of the ablated species with the background gas molecules or atoms and the influence of the gas pressure on the plume expansion process. This involves the comparison of the plume expansion process in reactive (oxygen) and inert (argon) atmospheres. Whereas in the former case chemical reactions may occur in the gas phase, only collisional interactions are possible in the latter.

II. EXPERIMENT

An ArF excimer laser beam [$\lambda = 193$ nm, pulse duration = 12 ns full width at half-maximum (FWHM)] is focused at an incidence angle of 45° on a rotating BiSrCaCuO (4334) target placed in a vacuum chamber evacuated to a residual pressure of 3×10^{-8} mbar. The laser fluence was fixed to 2.4 J/cm^2. Either oxygen or argon environments, with pressures ranging from 10^{-3} to 1 mbar, are introduced in the chamber in order to study their influence on the plasma expansion dynamics.

The plasma formed during the laser ablation process is imaged onto the entrance slit of a spectrometer (SPEX, 0.05 nm resolution), with ×2 magnification. The optical image of the plume is scanned along the normal to the target with a spatial resolution of 60 μm. The light emitted is collected by a photomultiplier (15 ns rise time) connected to a boxcar averager for spectrum recording or to a 500 MHz digitizer for transient emission measurements. Further details of the experimental setup have been published elsewhere.[10,11]

III. RESULTS

The emission spectrum has been studied in the 390–600 nm range and it has been recorded at a distance of 2 mm from the target in order to avoid the contribution of the continuum emission corresponding to the electrons that overlaps the emission of the excited species at distances to the target shorter than 1 mm.[10,11] It consists of a large number of spectral lines, most of them being identified according to standard tabulations.[12] They correspond both to neutrals (Bi*, Sr*, Ca*, and Cu*) and ions (Ca^{+}* and Sr^{+}*). No emission lines related to Bi^{+}* and Cu^{+}* were found. Although a specific search was performed for emission lines of oxidized diatomic species, both in vacuum and in oxygen, no emission lines from these molecules could be identified. This search included the following lines: 586.9 nm (BiO*); 384.8, 420.5,

a)Electronic mail: cnafonso@pinar1.csic.es

 0021-8979/95/77(12)/6588/6/$6.00

TABLE I. Transitions and energies of the upper and lower levels responsible for the emission lines studied in this work.

Species	Wavelength	Transition	Energy	
			Upper level (eV)	Lower level (eV)
Ca^+	396.85	$4p\ ^2P_{1/2} \rightarrow 4s\ ^2S_{1/2}$	3.12	0
Sr^+	416.18	$6s\ ^2S_{1/2} \rightarrow 5p\ ^2P_{1/2}$	5.91	2.98
Sr^+	421.55	$5p\ ^2P_{1/2} \rightarrow 5s\ ^2S_{1/2}$	2.98	0
Ca	422.68	$4p\ ^1P_1 \rightarrow 4s^2\ ^1S_0$	2.93	0
Ca	428.30	$4p^2\ ^3P_2 \rightarrow 4p\ ^3P_1$	4.78	1.89
Sr	460.73	$5p\ ^1P_1 \rightarrow 5s^2\ ^1S_0$	2.69	0
Bi	472.22	$7s\ ^4P_{1/2} \rightarrow 6p^3\ ^2D_{3/2}$	4.04	1.42
Sr	474.19	$5p^2\ ^3P_1^0 \rightarrow 5p\ ^3P_0^0$	4.41	1.80
Cu	510.55	$4p\ ^2P_{3/2} \rightarrow 4s^2\ ^2D_{5/2}$	3.82	1.39

and 598.3 nm (CaO*); 462.5, 470.9, and 474.9 nm (CuO*); 404.8, 593.8, 595.0, and 596.9 nm (SrO*), which were identified according to standard tabulations[13] or from the data previously reported in the literature.[14] Table I summarizes the lines selected for this study, their responsible electronic transition, and the energy of the upper and lower levels of the considered transitions.

No new lines appear when ablation takes place in oxygen or argon environments, compared to the spectrum recorded in vacuum, the enhancement of the emission intensities being the unique new feature observed. This relative enhancement depends not only on the gas background pressure and nature but mainly on the excitation energy of the electronic transition responsible of the emission line. Electronic transitions with excitation energies above 3 eV show a slight increase of the emission intensity, while the emission corresponding to transitions with excitation energies below this value shows instead a strong increase. Since the emission transients of ions (Ca^+* and Sr^+*) and neutrals (Bi*, Sr*, Ca*, Cu*) show similar features under all the experimental conditions studied, we have selected three calcium emission lines to show the representative results: Lines at 396.85 nm (Ca^+*) and at 422.68 nm (Ca*) with excitation energies ≈3 eV and a line at 428.30 nm (Ca*) that corresponds to a transition with an excitation energy ≈5 eV.

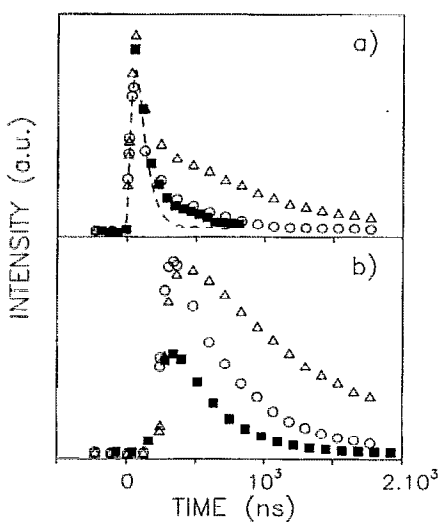

FIG. 1. Real-time emission intensity from the Ca* transition at λ=422.68 nm recorded at (a) 0.5 and (b) 3.35 mm from the target surface. The emission is recorded in vacuum (■), 1 mbar of oxygen (○), and 1 mbar of argon (△). The dashed line corresponds to the continuum emission recorded at λ=423.4 nm out of any identified line.

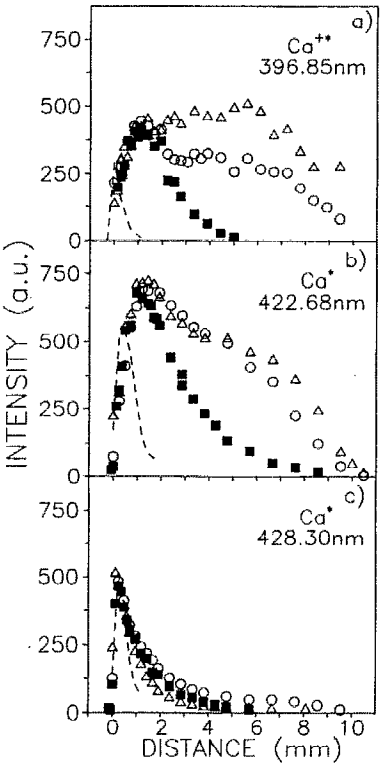

FIG. 2. Maximum emission intensity from (a) Ca^{+*} and (b),(c) Ca* transitions as a function of the distance to the target. Results are recorded in vacuum (■), 1 mbar of oxygen (○), and 1 mbar of argon (△). The dashed line corresponds to the continuum emission recorded at λ=423.4 nm out of any identified line. Results obtained from Ca* transitions with excitation energies of (b) ≈3 and (c) ≈5 eV are both included.

Figure 1 shows the emission transients corresponding to the emission line 422.68 nm (Ca*) recorded at two different distances d to the target surface and in different gas environments. The contribution of the continuum emission recorded in the neighborhood of the emission line but out of it (423.4 nm) is also shown. At short distances to the target (d=0.50 mm) [Fig. 1(a)], the transients show two contributions, the less delayed one behaving similarly to that of the continuum emission. The longer delayed and broader one is related to the emission due to the $4p\ ^1P_1 \rightarrow 4s^2\ ^1S_0$ Ca* transition.[12] At longer distances (>1 mm) there is no contribution of the continuum emission and only the emission from the Ca* transition is recorded, showing an increase of its intensity when a gas environment (either Ar or O_2) is present, as it is seen in Fig. 1(b) for d=3.35 mm.

Figure 2 shows the dependence of the transient emission intensity maximum on the distance to the target surface for the three considered transitions and the continuum contribution. The data were collected in three different environments: vacuum (3×10^{-8} mbar), 1 mbar of Ar, and 1 mbar of oxy-

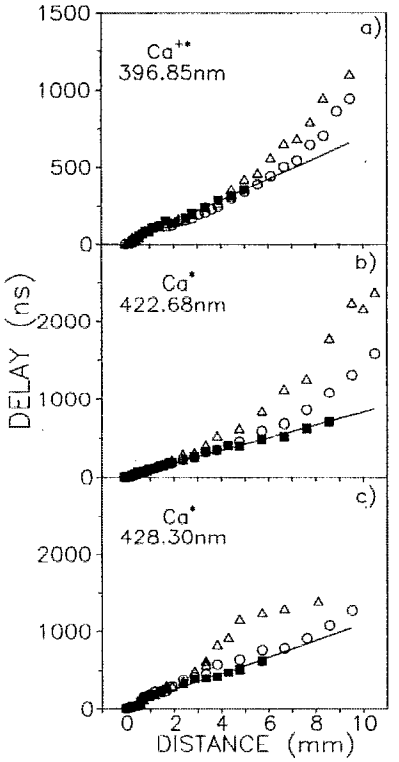

FIG. 3. Delay with respect to the laser pulse of the maximum emission intensity from (a) Ca^+* and (b),(c) Ca* transitions as a function of the distance to the target. Results are recorded in vacuum (■), 1 mbar of oxygen (○), and 1 mbar of argon (△). The solid line corresponds to the linear fit of the results recorded in vacuum. Results obtained from Ca* transitions with excitation energies of (b) ≈3 and (c) ≈5 eV are both included.

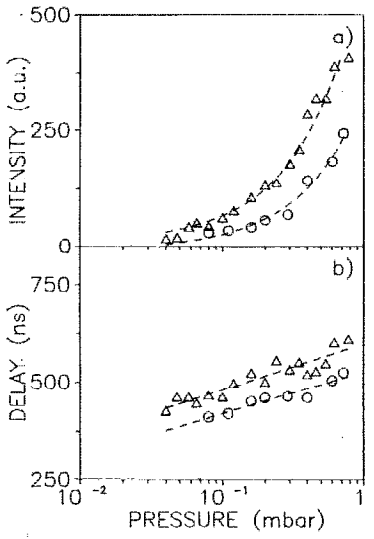

FIG. 4. (a) Maximum emission intensity and (b) delay with respect to the laser pulse from Ca^+* transition at λ=396.85 nm, as a function of the gas background pressure both in Ar (△) and in O_2 (○). The transients are recorded at 6.1 mm from the target surface. Lines are a guide for the eye.

gen. The contribution of the continuum emission to the total emission that can be observed in Fig. 1 and the results presented in Fig. 2 strongly suggest that the emission corresponding to the transitions studied is masked by the continuum emission in the region $0<d<0.5$ mm. When comparing the emission of the species in vacuum and in a gas environment it is possible to distinguish clearly two regions as a function of distance. For $0\leqslant d\leqslant 1.5$ mm the emission intensity has the same general behavior in all the environments studied, showing a maximum at a distance of 0.7–1 mm to the target surface followed by a decay tail in vacuum. At larger distances ($2\leqslant d\leqslant 10$ mm) the emission intensity depends on both the nature of the background gas and the electronic transition studied. In the presence of a gas background (either Ar or O_2) the emission intensity from the 396.85 nm (Ca^+*) and 422.68 nm (Ca*) lines show an important enhancement in respect to the intensities recorded in vacuum [Figs. 2(a) and 2(b)] as opposed to the 428.30 nm (Ca*) emission line. It shows no significant intensity enhancement although it can be recorded at longer distances, as can be seen in Fig. 2(c).

The time delay between the laser pulse and the transient emission intensity maximum versus the distance to the target surface is plotted in Fig. 3 for the three considered transitions. For distances to the target surface larger than 1 mm, where the continuum emission becomes negligible, the delay of the transient emission intensity maximum recorded in vacuum presents a linear dependence on the distance. The extrapolation of this linear dependence to $d=0$ leads to a delay t_0 of 20–30 ns for Ca^+*. This delay has to be understood in part as the time between the arrival of the maximum of the laser pulse to the target surface and the ejection of the material, and in part as a consequence of the use of emission spectroscopy techniques since it is necessary to wait a time of the order of the lifetime of the excited state to have optical emission. The most probable velocity of the species can be estimated from the inverse of the slope of this line.[9–11] Similar delay features are found in all the emitting species studied, and the calculated velocities, in the linear region, are in the range of $8-16\times10^5$ cm/s except for Sr^+ (20×10^5 cm/s). The velocity of ions is always found to be higher than that of the corresponding neutrals. When a gas background (either Ar or O_2) is introduced in the ablation chamber the delay is longer than that expected from a linear dependence for $d\geqslant 5$ mm, and this shift in the delay is longer for Ar than for O_2.

Since the presence of a gas pressure has a significant influence on the plasma expansion at large distances from the target (Figs. 2 and 3), the dependence of the transient emission intensity maximum and its delay with respect to the laser pulse on the gas pressure are analyzed at a fixed distance of 6.1 mm to the target. This distance is selected since the emission intensity presents there a maximum when a gas environment is present and the emission intensity in vacuum is almost negligible (see Fig. 2). Figure 4 shows the results obtained for the Ca^+* emission line. The 422.68 nm Ca* line shows a behavior similar to that of Ca^+*, while the emission intensity corresponding to the 428.30 nm Ca* line at this distance is below the experimental resolution in the studied pressure range. For gas pressures below 3×10^{-2} mbar (either in Ar or O_2) both the intensity [Fig. 4(a)] and the delay [Fig. 4(b)] are similar to those recorded in vacuum. For pres-

sures above 3×10^{-2} mbar, a sharp increase of the emission intensity is observed in both cases [Fig. 4(a)], whereas the time delay [Fig. 4(b)] increases slowly with pressure. These increases are always higher in Ar than in O_2 as we have previously observed in the space-resolved measurements (Figs. 2 and 3).

IV. DISCUSSION

The continuum emission observed in the neighborhood of the target surface (Fig. 1) suggests the existence of a high density of excited electrons in this region at the early stages of the plasma expansion. These electrons are in part responsible for the excitation of the ejected species via electron-impact processes.[8,15] As the plume expands in vacuum, their density, and therefore the probability of excitation of the ejected species, decreases. Then the emission intensity decreases and becomes zero at distances of a few mm from the target surface, as it is shown in Fig. 2 for calcium species.

The presence of a gas background during laser ablation (either Ar or O_2) has a strong influence on the plasma expansion process. The emission intensity increases significantly for gas pressures higher than 3×10^{-2} mbar [Fig. 4(a)] and distances to the target higher than 2 mm (Fig. 2) for emission lines with low excitation energy. The lifetime of the excited state of the studied transitions is in all cases of the order of a few ns,[13] while the observed increase of emission occurs at times of the order of hundreds of ns. Therefore, this increase of emission should correspond to species that have been excited during plasma expansion through two main processes: particle collisional excitation and electron-impact excitation/recombination.[4,8,15,16] Since the cross section of the former is about two orders of magnitude smaller than that of the latter,[15,16] electron-impact processes are most likely responsible for the excitation of the species as the plume expands, the electrons being produced by ionization of the foreign species. Since the ionization potential of the two considered gases is 15.7 eV for Ar and 12.5 eV for O_2,[17] a higher electron density is expected in an O_2 environment according to the above-mentioned excitation process and a higher emission intensity should be expected in this environment. The experimental results presented in Figs. 2 and 4(a) show instead a higher emission intensity in the case of an Ar environment; therefore, there has to be another process that favors the excitation of the ejected species in Ar environment. It is known that the presence of a foreign gas produces a plasma confinement[4,15] and consequently an increase of the density of the ejected species in the plume, the higher the mass of the foreign gas the higher the confinement and therefore the higher density of ejected species and the higher probability of excitation. Since Ar is heavier than O_2 the confinement should be stronger in Ar thus leading to a higher optical emission as experimentally observed.

The fact that the delay increases linearly with the distance to the target surface in vacuum, suggests a free expansion of the plasma.[15,18] The presence of a gas background produces a nonlinear dependence of the delay on the distance to the target for $d>5$ mm (Fig. 3) and on the pressure for pressures higher than 3×10^{-2} mbar [Fig. 4(b)]. This behavior is consistent with a slowing down of the ejected species

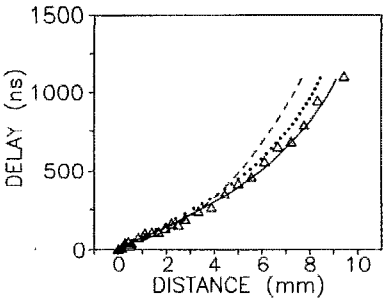

FIG. 5. Experimental values (△) of the delay with respect to the laser pulse of the maximum emission intensity from the Ca^{+}* transition at $\lambda=396.85$ nm, as a function of the distance to the target in 1 mbar of Ar. The dashed line shows the best fit obtained with the shock wave model [$t=k'(d+d_0)^{5/2}$, with $k'=(p/k)^{1/2}$ and $k'=0.589$ ns/mm$^{5/2}$, $d_0=2.03$ mm]. The solid line shows the best fit achieved by the drag model [$t=d_f(1-e^{-\beta t})-d_0$, with $d_f=11.6$ mm, $\beta=15.2\times10^{-4}$ ns, and $d_0=0.32$ mm]. The points ($\cdots$) correspond to the simulation obtained in the frame of the drag model using the experimental values of v_0 (16.2×10^6 mm/s) and t_0 (22 ns, which leads to $d_0=0.35$ mm) and the value of β (14.9×10^{-4} ns) obtained from Fig. 7 for 1 mbar of Ar.

velocity in the presence of a foreign gas both for large distances to the target and for high gas pressures. A shock wave model has been proposed[19,20] to describe the plasma expansion dynamics in the presence of a gas background at pressures higher than ≈1 mbar. According to this model the motion can be described by an ideal blast wave in which

$$d=(k/p)^{1/5}t^{2/5}, \tag{1}$$

where d is the distance to the target surface, k is a constant proportional to the laser energy density, p is the gas background pressure, and t is the time at which the maximum of the transient emission is observed.

As it has been pointed out above, it is necessary to wait a certain amount of time t_0 to have emission at $d=0$. This boundary condition can be introduced in the above equation as a constant term d_0 as follows:

$$d=(k/p)^{1/5}t^{2/5}-d_0. \tag{2}$$

The best fit for the delay of the maximum intensity, calculated using this model for Ca^{+}* at 1 mbar of Ar, as a function of the distance to the target is plotted in Fig. 5 together with the experimental data. It is seen that the calculated values do not fit the experimental results very well, especially for large distances ($d>4$ mm). The above formula also allows one to calculate the dependence of the delay on the pressure for a fixed distance. The results from the calculations together with the experimental results for Ca^{+}* at 1 mbar of Ar are included in Fig. 6 where it is seen that the agreement between calculated and experimental results is now very poor.

At pressures lower than ≈1 mbar, the collisions between the ejected species and the background gas leading to the slowing down observed in Fig. 3 have been explained in terms of the elastic scattering of the ejected species by the atoms or molecules of the background gas.[21] In that case, the slowing down can be accounted for by a classical drag force model[6] as that proposed by Geohegan[5,22] to predict the early

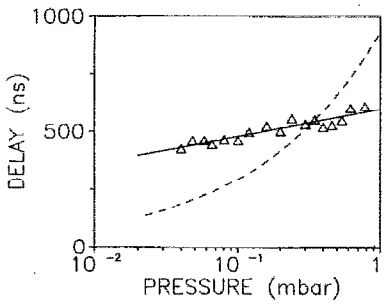

FIG. 6. Delay with respect to the laser pulse of the maximum emission intensity from the Ca^{+*} transition at $\lambda=396.85$ nm, as a function of the argon pressure (△) at 6.1 mm from the target surface. The dashed line shows the fit obtained with the shock wave model ($t=k''p^{1/2}$, with $k''=[(d+d_0)^5/k]^{1/2}$ and $k''=943$ ns/mbar$^{1/2}$). The solid line shows the fit of the experimental results to a logarithmic function [$t=A\ \ln(p)+B$, with $A=51.3$ ns and $B=480$ ns].

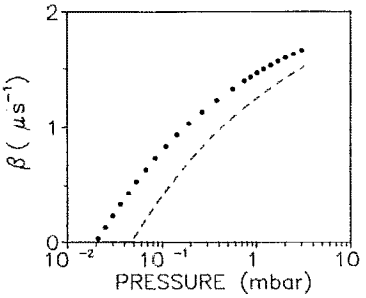

FIG. 7. Empirical dependence of the slowing coefficient β on the pressure of the background gas for oxygen (· · ·) and argon (dashed line) obtained in the frame of the drag model using the logarithmic fit of the dependence of the delay on pressure shown in Fig. 6.

stages of plasma expansion at short distances to the target. The ejected species are considered as an ensemble which experiences a viscous force proportional to its velocity through the background gas. In this situation the plume expansion can be expressed as

$$d=d_f[1-\exp(-\beta t)]-d_0, \tag{3}$$

where d and t have the same signification as in the shock wave model, β is the slowing coefficient that depends on the pressure and nature of the gas environment, $d_f=v_0/\beta$ is the stopping distance of the plume, and v_0 is the initial velocity of the ejected species. Similarly to what has been pointed out for the shock wave model [Eq. (2)], we have added the constant term d_0 as a boundary condition related to the experimental technique used.

Figure 5 shows also the results obtained using the drag model, and an excellent agreement is seen between the calculated and the experimental values. The best fit was achieved with $d_f=11.6$ mm, $\beta=15.2\times10^{-4}$ ns^{-1}, and $d_0=0.32$ mm which led to a value of $v_0=17.6\times10^3$ m/s and $t_0=18$ ns. These values are in good agreement with the experimental ones obtained in the linear region ($v_0=16.2\times10^3$ m/s and $t_0=22$ ns). It can be then concluded that the drag model predicts quite accurately the plasma expansion in the region where emission intensity could be recorded ($d<10$ mm). In order to give further support to this conclusion, the drag model should also fit well the experimental data of the delay as a function of pressure. The coefficient β depends on the pressure although no explicit dependence was found in the literature. Equation (3) allows us to express β as a function of time, and the experimental results included in Fig. 4(b) show an approximately linear dependence between the delay time and $\ln(p)$ [$t=A\ \ln(p)+B$]. Combining both expressions, it has been possible to establish the functional dependence shown in Fig. 7 for the coefficient β on the pressure of argon and oxygen environments.

The consistency of the values calculated for β was tested by simulating the dependence of the delay time on the distance for a given pressure, starting from the values of v_0 and t_0 obtained in vacuum and the β value corresponding to 1 mbar of Ar (Fig. 7). The results obtained are also included in Fig. 5 and it is clearly seen that although the calculated results are similar to the experimental ones, the delays are slightly shifted to higher values at large distances to the target. Since it has been earlier reported that the angular scattering of the ejected species depends on the ratio of the mass of the ejected to gas environment species,[21] the small divergence between calculated and experimental results shown in Fig. 5 may be related to the fact that the nature of the foreign gas has not been explicitally taken into account in the model. Similar calculations were also performed for an Ar pressure of 10^{-1} mbar and for O_2 pressures of 10^{-1} and 1 mbar. Since the agreement between calculated and experimental results is always very good, it can be then concluded that the drag model explains quite well the observed dependence of the intensity and the delay of the emission on the gas pressure and the distance to the target surface.

Reactive processes have been widely reported in YBaCuO ablation experiments[4,5,7,9] and explained in terms of the formation of oxidized species during plasma expansion.[6] The oxidation of Y or Ba to form YO or BaO species is an exothermic process as opposed to what happens with Bi, Sr, Ca, and Cu species which form oxidized species through endothermic processes as shown in Table II.[6,23] This reasoning is in good agreement with the lack of experimental evidence of the formation of oxide molecules during the plasma expansion in laser ablation of BiSrCaCuO in oxygen observed both in this work and in earlier works.[14] Since similar qualitative and quantitative results are obtained for reactive (O_2) and inert (Ar) environments, the excitation and

TABLE II. Reaction exothermicities (in eV) for the formation of monoxide species. The values are estimated according to the model proposed in Ref. 6 from the values of the dissociation energies of monoxides presented in Ref 23. The negative sign indicates that the reaction is endothermic.

Monoxides	Energy (eV)
CuO	−2.36±0.22
BiO	−1.62±0.13
SrO	−0.99±0.17
CaO	−0.74±0.17
BaO	0.67±0.14
YO	2.29±0.11

the slow-down mechanisms in O_2 should be very similar to those described above for an Ar environment, i.e., electron-impact excitation and elastic scattering, respectively. The influence of reactive processes on the plasma expansion at the distances and pressures studied in the presence of an O_2 background has then to be negligible.

Finally, it has been shown in Figs. 2 and 3 that the Ca* and Ca^{+}* lines due to electronic transitions with excitation energies $\approx$3 eV present the same behavior and their features are quite well explained within the frame of the drag model. The emission line at 428.30 nm (Ca*) which involves electronic transitions with an excitation energy of $\approx$5 eV showed no significant increase of the emission intensity for $d \geq 1.5$ mm as opposed to what has been observed for the other Ca* and Ca^{+}* emission lines. The lines studied for the other ejected species present similar features. Emission lines such as Sr^{+}* (421.55 nm) and Sr* (460.73 nm), involving transitions with energies of excitation of the order of 2.7–3 eV show a behavior similar to that observed for Ca^{+}* (396.8 nm) and Ca* (422.7 nm). The Bi* (472.2 nm), Sr* (474.19 nm), and Cu* (510.55 nm), with high excitation energies (3.8–5 eV) show features similar to those of the Ca* (428.30 nm) transition. These results are consistent with a low efficiency in populating high-energy electronic excited levels as it has been proposed by Fried *et al.*[7]

The Sr^{+}* (416.18 nm) emission line, which involves an excited state with an energy of excitation of 5.91 eV, shows an increase of its emission intensity when ablation is performed in a gas environment (either Ar or O_2). Although this result seems to be in disagreement with the above explanation, the fact that Sr^{+} ions have the highest velocity in the plume (20×10^3 m/s) might explain this anomaly. This velocity leads to a kinetic energy around 175 eV, which is much higher than that of the other studied species which are in the 25–100 eV range. The front of the plume should be then mainly formed by Sr^{+} ions. Since the electron density and the available energy are much higher in this region, excitation processes involving these energetic ions can then become effective to populate electronic states with high energy of excitation.

V. CONCLUSION

This work shows clearly that the presence of an atmosphere during laser ablation of BiSrCaCuO modifies the plume expansion dynamics for pressures higher than 3×10^{-2} mbar. The similar behavior observed in the expansion process in reactive (O_2) and inert (Ar) atmospheres suggest that the dominant interaction processes between the ablated species and the gas molecules or atoms should be the same and, due to the nonreactive nature of Ar, they should be mainly collisional. A classical drag model is shown to describe quite accurately the experimental results related to the expansion process and an empirical dependence for the slowing coefficient β on the gas pressure could be obtained. Finally, the different degree of enhancement of the emission intensity observed in the different studied lines is related to the different excitation energies of the upper levels involved in the considered transition. It is concluded that transitions involving excitation energies $\leq$3 eV have to be studied in order to analyze properly the plume expansion.

ACKNOWLEDGMENTS

This work was partially supported by the SCIENCE project SCT-910753. Dr. J. Perrière (Université Paris VII and VI, France) is thanked for providing the target and for stimulating discussions. Dr. J. Solís (I. Optica, Spain) is thanked for helpful discussions. One of us (J.G.) acknowledges a FPI grant from the Spanish Ministry of Educación y Ciencia.

[1] D. Dijkkamp, T. Venkatessan, X. D. Wu, S. A. Shasheen, N. Jisrawi, Y. H. Min Lee, W. L. McLean, and M. Croft, Appl. Phys. Lett. **51**, 619 (1987).
[2] K. L. Saenger, Proc. Adv. Mater. **2**, 1 (1993).
[3] J. Perrière, in *Laser Ablation of Electronic Materials: Basic Mechanism and Applications* (North-Holland, Amsterdam, 1992), p. 293.
[4] H. F. Sakeek, T. Morrow, W. G. Graham, and D. G. Walmsley, J. Appl. Phys. **75**, 1140 (1994).
[5] D. B. Geohegan, Thin Solid Films **220**, 138 (1992).
[6] A. Gupta, J. Appl. Phys. **73**, 7877 (1993).
[7] D. Fried, G. P. Reck, T. Kushida, and E. Rothe, J. Appl. Phys. **70**, 2337 (1991).
[8] H. S. Kwok, Thin Solid Films **218**, 277 (1992).
[9] W. Marine, M. Gerri, J. M. Scotto d'Aniello, M. Sentis, Ph. Delaporte, B. Forestier, and B. Fontaine, Appl. Surf. Sci. **54**, 264 (1992).
[10] F. Vega, C. N. Afonso, and J. Solis, J. Appl. Phys. **73**, 2472 (1993).
[11] J. Gonzalo, F. Vega, and C. N. Afonso, Thin Solid Films **241**, 96 (1994).
[12] W. F. Heggers, C. H. Corliss, and B. F. Scribner, NBS Monograph 145, 1975; C. E. Moore, NSRDS-NB Monograph 35, 1971.
[13] A. A. Radzig and B. M. Smirnov, *Reference Data on Atoms, Molecules and Ions* (Springer, Berlin, 1985); R. W. Pearse and A. G. Gaydon, *The Identification of Molecular Spectra* (Wiley, New York, 1976).
[14] C. Girault, D. Damiani, C. Champeaux, P. Marchet, J. P. Mercurio, J. Aubreton, and A. Catherinot, Appl. Phys. Lett. **56**, 1472 (1990).
[15] H. P. Gu, Q. H. Lou, N. H. Cheung, S. C. Chen, Z. Y. Wang, and P. K. Liu, Appl. Phys. B **58**, 143 (1994).
[16] C. Timmer, S. K. Srivastava, T. E. Hall, and A. Fucaloro, J. Appl. Phys. **70**, 1888 (1991).
[17] *Handbook of Chemistry and Physics*, 62nd ed. (CRC, Boca Raton, FL, 1981).
[18] P. E. Dyer, R. B. Greenough, A. Issa, and P. H. Key, Appl. Phys. Lett. **53**, 534 (1988).
[19] P. E. Dyer, A. Issa, and P. H. Key, Appl. Phys. Lett. **57**, 186 (1990).
[20] W. K. A. Kumuduni, Y. Nakayama, Y. Nakata, T. Okada, and M. Maeda, J. Appl. Phys. **74**, 7510 (1993).
[21] J. C. S. Kools, J. Appl. Phys. **74**, 6401 (1993).
[22] D. B. Geohegan, Appl. Phys. Lett. **60**, 2732 (1992).
[23] Values derived using the dissociation energies of monoxides from J. B. Pedley and E. M. Marshall, J. Phys. Chem. Ref. Data **12**, 967 (1983).